Salinity causes widespread restriction of methane emissions from inland waters

Cynthia Soued (cynthia.soued@gmail.com)
University of Lethbridge https://orcid.org/0000-0003-1985-7672
Kerri Finlay
University of Regina
Lauren Bortolotti
Ducks Unlimited Canada
Sydney Jensen
University of Regina
Peter Leavitt
University of Regina https://orcid.org/0000-0001-9805-9307
Peka Mueller
University of Lethbridge
Björn Wissel
Université Claude Bernard Lyon 1
Matthew Bogard
University of Lethbridge

Article

Keywords:

Posted Date: June 30th, 2022

DOI: https://doi.org/10.21203/rs.3.rs-1762660/v1

Salinity causes widespread restriction of methane emissions from inland waters

Cynthia Soued[1*], Kerri Finlay[2, 3], Lauren E. Bortolotti[4], Sydney Jensen[2], Peter R. Leavitt[3,5], Peka Mueller[1], Björn Wissel[3,6], Matthew J. Bogard[1]

[1] Department of Biological Sciences, University of Lethbridge, Lethbridge, AB Canada

[2] Department of Biology, University of Regina, Regina, SK Canada S4S 0A2

[3] Institute of Environmental Change and Society, University of Regina, Regina, SK S4S 0A2

[4] Institute for Wetland & Waterfowl Research, Ducks Unlimited Canada, PO Box 1160 Stonewall, MB, Canada R0C 2Z0

[5] Limnology Laboratory, Department of Biology, University of Regina, Regina, SK S4S 0A2

[6] LEHNA, Université Claude Bernard Lyon 1, 69622 Villeurbanne Cedex, France

[*]Corresponding author: Dr. Cynthia Soued

Inland waters are the largest natural source of methane (CH_4), a potent greenhouse gas, but models and estimates of aquatic CH_4 cycling and emissions were developed in soft-water ecosystems and may not apply to globally abundant salt-rich inland waters. Here we show that elevated salinity constrains microbial CH_4 cycling restricting aquatic emissions at large scales. Our survey of the Canadian Prairie ecozone demonstrates that salinity interacts with organic matter availability to shape CH_4 patterns across aquatic networks (rivers, lakes, wetlands, and agricultural ponds). Current empirical models, biased toward solute-poor surface waters, overestimated CH_4 concentrations and emissions measured in hardwater systems by up to several orders of magnitude, with discrepancies strongly linked to salinity. Models were particularly inaccurate for bubble-mediated emissions from small lentic systems, one of the largest sources of aquatic CH_4 globally. Elevated salinity reduced aquatic CH_4 emissions by an estimated 81 % in the Canadian Prairies, and could result in a 7.8 % overestimation of global lentic emissions. Widespread salinization of inland waters under future land use and climate regimes could further restrict methane emissions.

Methane (CH_4) is a potent greenhouse gas responsible for 16 % of current atmospheric radiative forcing[1]. Inland waters are the largest natural source of CH_4 globally, emitting 398.1 (±79.4) $TgCH_4$ yr^{-1} [2,3]. However, this number is largely based on measurements performed in solute-poor waters[2,4–6], despite salt-rich systems representing nearly half of the global inland water volume[7]. There is increasing evidence to suggest that salinity, particularly as sulfate (SO_4^{2-}), inhibits CH_4 production through multiple mechanisms, which may lead to lower CH_4 emissions from these systems[8–11]. The paucity of empirical data from salt-rich inland waters raises questions

about our current understanding of aquatic CH_4 regulation, and about the accuracy of global emissions estimates.

The salinity of aquatic ecosystems shapes microbial communities[12], in particular the abundance and distribution of methanogens and methanotrophs[13,14]. Methanogenesis is the least energy-efficient carbon (C) mineralization process in the redox chain. An abundance of ions favors more energetically efficient reactions, with sulfate (SO_4^{2-}) and iron (Fe^{3+}) reducers outcompeting methanogens for labile C substrate and hydrogen ions[11,15,16]. The reduction of SO_4^{2-}, nitrate (NO_3^-), and Fe^{3+} ions can be coupled to anaerobic CH_4 oxidation[17–23], further supressing ambient CH_4 concentrations at high salinity levels. Salinity can also interact with other key CH_4 controls, with organic C availability modulating the SO_4^{2-} inhibition of methanogenesis[11,18,24,25], and nutrient availability changing with salt content due to sorption to sediments[18,26]. Salinity thus integrates multiple pathways of CH_4 suppression. The inhibition of CH_4 by salinity (especially SO_4^{2-}) has been demonstrated in coastal and salt-rich wetlands[9,10,27–31], as well as in one lacustrine experiment[8], suggesting a potentially significant effect on CH_4 across salt-rich inland waters. However, the impact of this fine-scale salt regulation on regional and global CH_4 emissions is unknown.

Here we survey 193 rivers, lakes, open-water wetlands, and agricultural ponds spanning a wide range in morphometry, hydrology, chemistry, and trophic status in the Canadian Prairies (Fig. 1 and Table S1), a region with the highest density of salt-rich inland waters worldwide[32]. We show that salinity is a key driver of CH_4, interacting with organic matter (OM) content to shape surface CH_4 partial pressure (pCH_4). Elevated salinity reduced CH_4 emissions in small lentic waterbodies, especially through ebullition, by an average of three-fold relative to predictions from existing freshwater models, representing a flux reduction comparable to major components of the regional

CH_4 budget. The negative effect of salinity on CH_4 emissions, that we also identified in other hardwater regions, could lower global lentic emissions by 7.8 %.

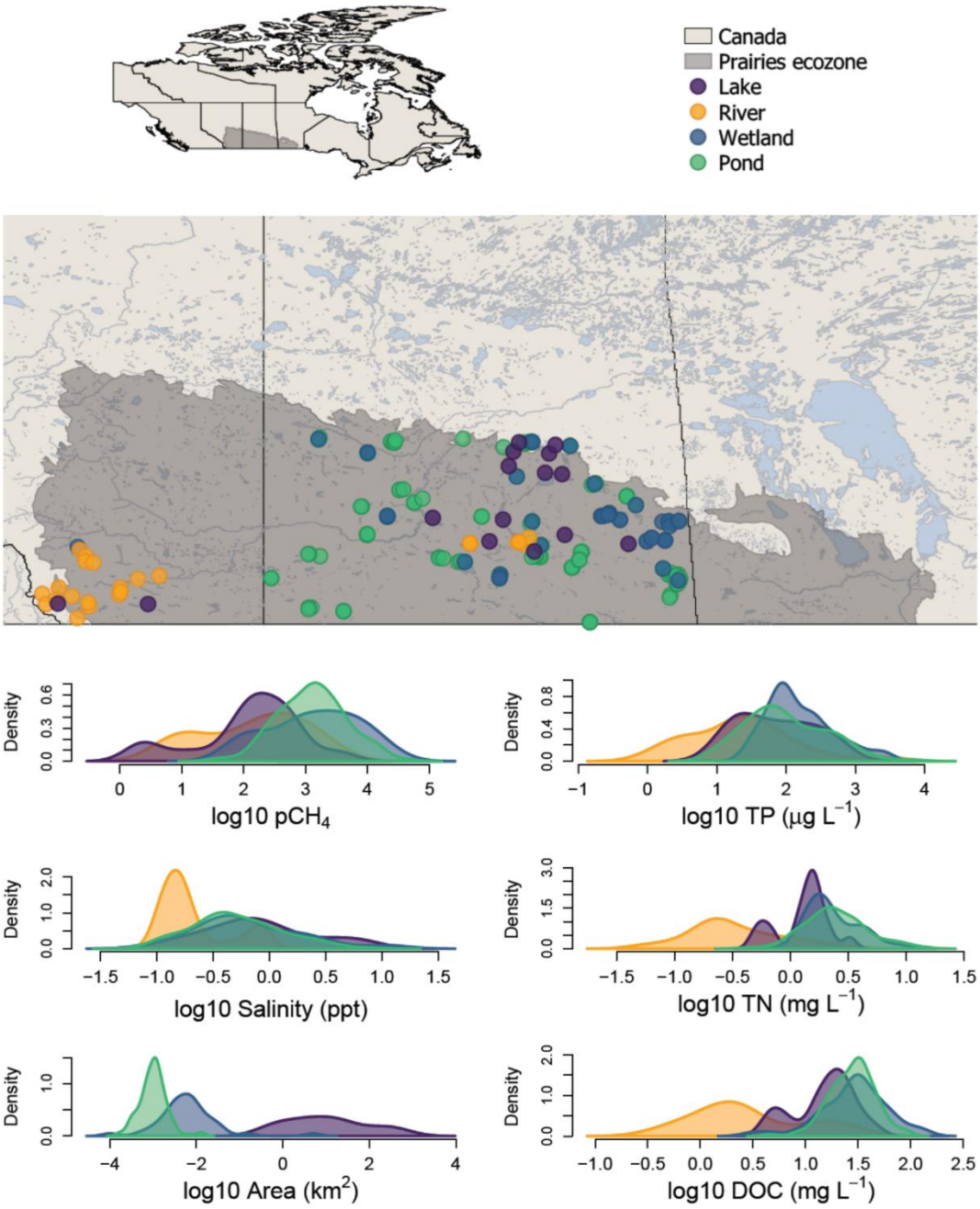

Fig. 1. Map of study area (Canadian Prairies) and sampled sites with density distribution plots of measured environmental properties by ecosystem type. See Table S1 for summary statistics.

Salinity-pCH_4 link varies across ecosystem types

Across all sampled sites, salinity had a strong negative effect on pCH_4 in a multiple linear regression that also included temperature[33–35], and common proxies for organic substrate (DOC and TP[4,5,36,37]) (Table S2 and Fig. S1 and S2). The effect of salinity on pCH_4 varied among ecosystem types, from non-significant in rivers and lakes, to pronounced control of pCH_4 in small lentic systems (surface area < 0.1 km^2, wetlands and agricultural ponds) (Table S2 and Figs. S1 and S2). In rivers, salinity, DOC, and nutrient concentrations were highly colinear (Pearson r > 0.6), making salt-rich rivers also highly concentrated in organic matter (elevated DOC and nutrient content), and overriding a potential inhibitory effect of salinity on pCH_4. Similarly, there was no significant influence of salinity in lakes (surface area > 0.1 km^2), whereas ionic concentration was a key pCH_4 predictor in small, often shallow, lentic waterbodies (Figs. S1 and S2). The enhanced effect of salinity in small and shallow waterbodies may reflect the closer connection between surface pCH_4 and sediments methanogenesis, directly affected by salinity, compared to larger lakes where pCH_4 is more susceptible to water column processes like mixing, oxidation, and pelagic production[38,39]. Importantly, the strong influence of salinity on pCH_4 observed in small lentic waterbodies (Fig. S1 and S2) has the potential for large-scale impacts as these wetlands and ponds are the most abundant aquatic features in the regional Prairie landscape[32,40,41] and a large source of CH_4 globally[2,3].

Interplay between salinity and OM regulates pCH_4

The positive correlation between pCH_4 and the DOC/salinity ratio (p-value << 0.001 and R^2_{adj} = 0.28, Fig. 2a) suggests that organic-rich systems (with elevated DOC concentrations) can compensate for the inhibitory effect of salinity on methanogenesis. pCH_4 correlated similarly with ratios of TN or TP to salinity, supporting the use of DOC as a proxy for OM content. This correlation, in line with previous research, likely reflects the absence of competition for organic substrate between methanogenesis and other reduction pathways (namely SO_4^{2-} reduction) when OM is abundant or when the low concentration of other electron acceptors limits alternative redox processes[11,18,24]. Conversely, low DOC/salinity ratios may favor alternative reduction reactions[11,15,16] that outcompete methanogens for the limited organic substrate, resulting in lower pCH_4. This inhibitory effect is likely mostly caused by SO_4^{2-} ions, which correlated strongly with salinity (Fig. S3), in line with previous studies of brine composition in Canadian Prairie waters[32]. Our data suggest that the fine-scale interplay between ion and organic matter content shapes pCH_4 patterns across the aquatic network at sub-continental scales.

OM availability and salinity have opposite effects on surface pCH_4, however, these two drivers are positively correlated (Pearson r = 0.52). The concentration of OM, nutrients, and ions often covary due to common catchment sources (e.g., agricultural and urban inputs), hydrological transport, and evapoconcentration[32,42–45]. Accordingly, the highest salinity, DOC, TP, and TN concentrations were found in lentic waterbodies with long water residence time (WRT) favoring solute accumulation, while fast-flowing lotic systems were the most solute-poor (Fig. 1 and Table S1). Site-specific factors can decouple OM and ions, with groundwater inputs, local geology, and atmospheric depositions changing ionic water composition[7,32,46], whereas internal metabolism independently regulates OM stocks[47]. This leads to a wide range in the ratio of DOC to salinity

observed in sampled sites (Table S1), that contribute to variance in pCH_4 within and across ecosystem types (Fig. 1 and 2).

Based on the empirical relationship in Fig. 2a, the modelled response of pCH_4 to changes in salt content is non-linear, with the greatest sensitivity at low end of the salinity gradient (Fig. 2b). The majority of sampled sites (78 %) in the Prairie landscape exhibited moderate salinity < 1 ppt (Fig. 1 and Table S1), a range within which even modest salinity changes from year to year[45,48] could have a substantial effect on CH_4 dynamics (Fig. 2b). For instance, at DOC = 10 mg L^{-1}, increasing salinity from 4 to 4.5 ppt is predicted to result in an 11% decrease in pCH_4 (from 51 to 46 ppm) compared to a 50% reduction (407 to 203 ppm) when increasing salinity from 0.5 to 1 ppt (Fig. 2b). The impact of doubling salinity at this level is comparable to that of halving the DOC concentration (Fig. 2b), highlighting the overlooked importance of salinity as a CH_4 control in the Canadian Prairie landscape.

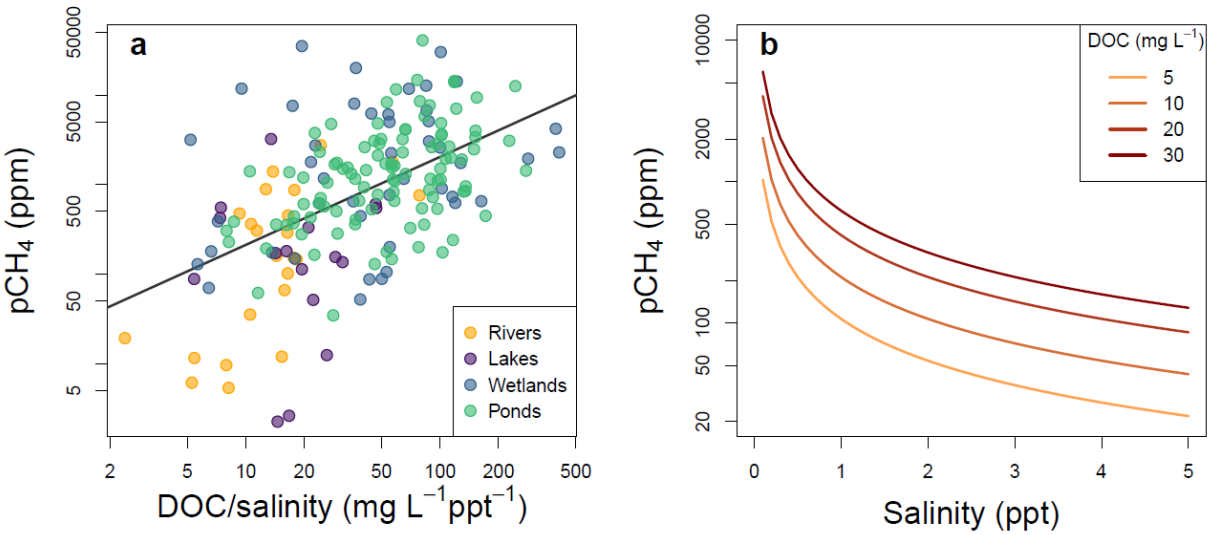

Fig. 2. a) Linear regression of pCH_4 (ppm) as a function of the DOC (mg L^{-1}) to salinity (ppt) ratio (p-value << 0.001, $R^2_{adj} = 0.28$, equation (with standard errors): $\log_{10}(pCH_4) = 1.34\ (\pm 0.19) + 0.98\ (\pm 0.11)\ \log_{10}$ (DOC / Salinity)). b) Modeled pCH_4 as a function of salinity at varying levels of DOC based on the empirical equation model from panel a.

Salinity lowers CH_4 emissions

Increased salinity lowered CH_4 emissions from inland waters in the Canadian Prairies and in two other salt-rich landscapes[49,50], particularly via ebullition from small lentic systems (Fig. 3). Diffusive CH_4 fluxes ranged from 0.11 to 91 mmol m^{-2} d^{-1} in Prairie wetlands and ponds (Fig. 3 and Table S1), within the global range reported in small (< 0.1 km^2) waterbodies[36]. Ebullitive CH_4 fluxes, measured in 10 sites (5 wetlands and 5 agricultural ponds), spanned 6 orders of magnitude, with 70 % of measurements lower than the 1st quantile of globally reported ebullition rates for small lentic systems[36]. Both diffusive and ebullitive flux rates were negatively correlated with salinity (Fig. 3), although the regression slope was much steeper for ebullition than for diffusion

(-3.0 vs -0.7, respectively, on a $\log_{10}$ scale), with a 10-fold increase in salinity (0.1 to 1 ppt) leading to a 4.5 vs 1000-fold decline in diffusion vs ebullition, respectively. The stronger influence of salinity on ebullition infers an impact on sediment CH_4 dynamics (CH_4 production and anaerobic oxidation), whereas water column CH_4 production, consumption, and physical mixing influence surface diffusion and weaken the effect of salinity on this flux pathway. Subsequent analysis of published data from lakes and ponds in Tibet and Mexico[49,50] (Fig. 3) further suggest that salinity could restrict aquatic CH_4 emissions from hardwater landscapes worldwide.

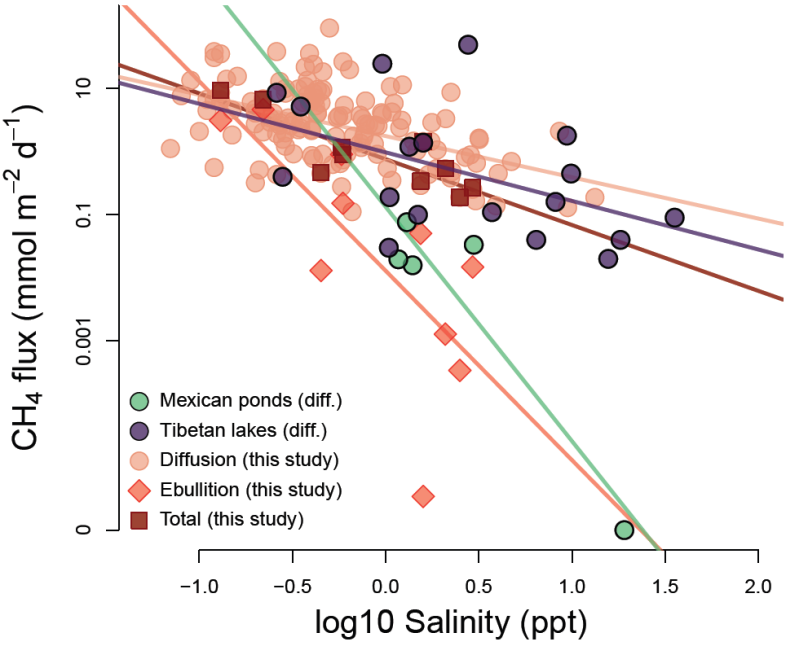

Fig 3. Negative relationship between salinity and lentic CH_4 emissions in different salt-rich landscapes. Data are from the Canadian Prairies (this study), the Tibetan Plateau (18 lakes[50]), and the Cuarto Cienegas Basin in Mexico (5 ponds[49]). Statistics of linear regressions are as follow: p-values = 0.04, << 0.001, 0.02, and 0.002; R^2_{adj} = 0.19, 0.25, 0.47, and 0.69; slope = -0.8, -0.7, -3.0,

and -1.0; and intercept = -0.01, 0.24, -1.9, and -0.12 (on log_{10} scales) for Tibetan lakes, and for diffusion, ebullition, and total flux from Canadian sites, respectively. No statistics are presented for the Mexican ponds since one of the flux values was zero and could not be log-transformed.

Existing empirical models[5,34,35,37] weakly predicted CH_4 dynamics in our study systems, and deviations from predictions were strongly linked to salinity (Fig. 5). The models we tested were developed based on regional and global data largely from freshwater systems[5,34,35,37], and use typical CH_4 drivers including water temperature, river discharge, lentic surface area, chlorophyll *a*, TN and DOC concentrations. These models captured a third of the observed variability in pCH_4 in our dataset (R^2 = 0.32; Fig. 4a), and only weakly predicted diffusive and ebullitive emissions from small lentic systems (R^2 = 0.15 and 0.03 respectively; Fig. 4b-c). Salinity, not included in these models, explained 20, 24, and 42 % of the deviation from predicted pCH_4, diffusion, and ebullition, respectively (Fig. 4d-f). Model deviation was particularly large for ebullitive fluxes in wetlands and agricultural ponds, being on average ~3 orders of magnitude lower than predicted (Fig 4c,f; in line with results from Fig. 3) reflecting a particularly strong impact of salinity on sediment-related processes. The inclusion of salinity in CH_4 models will therefore improve emissions estimates, particularly ebullition flux rates from small lentic systems.

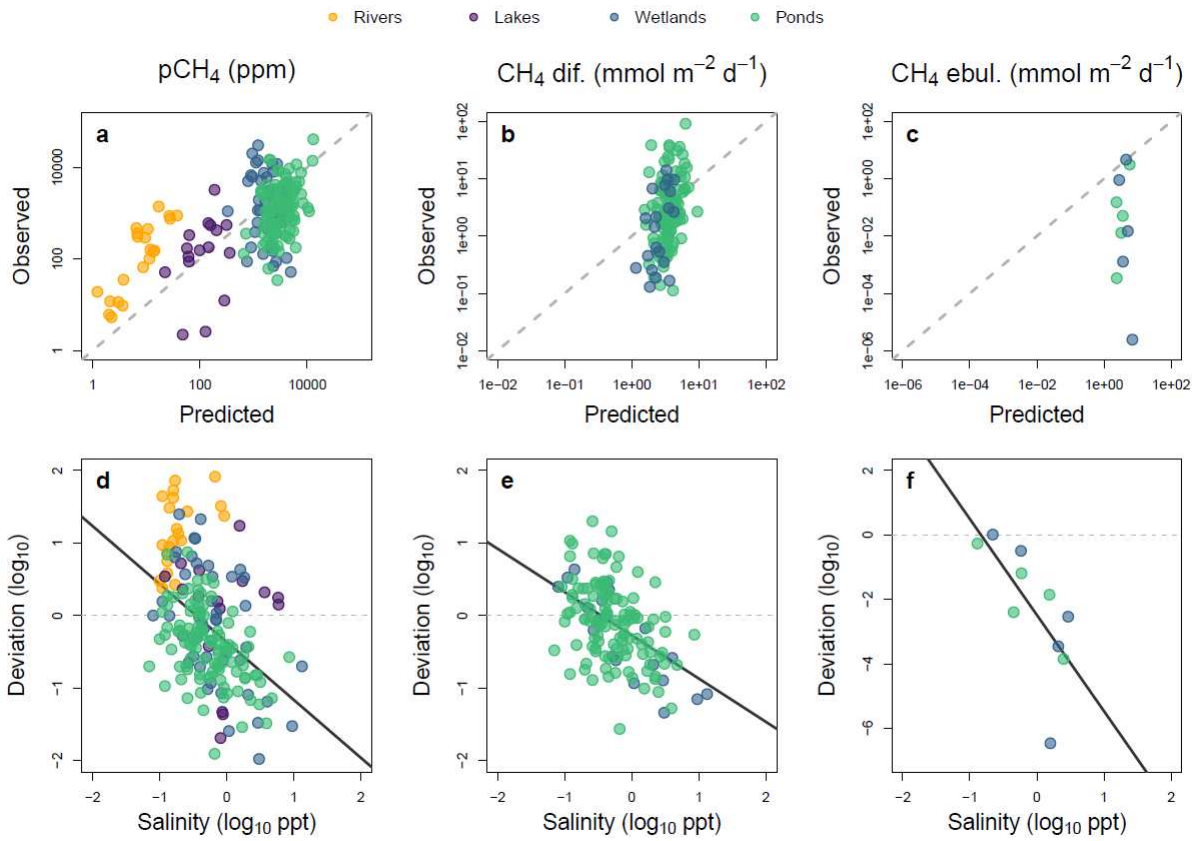

155

156 **Fig. 4.** Observed versus predicted (based on published models[5,34,35,37]) values of CH_4 partial
157 pressure (a), diffusion (b), and ebullition (c) in sampled sites, and the corresponding deviations
158 from predictions (measured - modeled) as a function of salinity (d-f). The grey dashed line
159 represents a perfect correspondence between predicted and observed values. Linear regression
160 lines (solid black) in d-f have p-values < 0.05, R^2_{adj} = 0.20, 0.24, and 0.42, and slopes = -0.80, -
161 0.60, and -3.0 for CH_4 partial pressure, diffusion, and ebullition, respectively.

162

Salinity impacts large-scale CH_4 budgets

Model simulation suggests that high salinity reduces total CH_4 emissions by ~5-fold from small lentic systems in the Canadian Prairies. We tested the effect of two salinity levels: 0.5 vs 0.1 ppt, respectively corresponding to the median of sampled small lentic sites (Table S1) vs a typical freshwater value, on the total (diffusion + ebullition) CH_4 emission rate based on the empirical relationship in Fig. 3. This yielded a large difference in flux rate (1.57 vs 8.42 mmol m^{-2} d^{-1}, respectively), consistent with the ~3-fold overestimation of total flux rates by existing freshwater models (Fig. 4). We applied this simulated difference in flux rate to three summer months and to a regional estimate of the area of small (< 0.1 km^2) lentic systems, totalling 2,869 km^2 in the Canadian Prairies. This resulted in a > 5-fold lower emissions in the actual salt-rich vs freshwater scenario (6,555 vs 35,169 Mg CH_4). This difference of 28,613 Mg of CH_4 (representing 0.97 $TgCO_2eq$) is regionally significant, equal, in terms of C footprint (CO_2 + CH_4 emissions), to ~11 % of the beef cattle industry of the province of Saskatchewan[51], or to the entire Canadian wastewater treatment sector[52].

Global CH_4 emissions from lentic waterbodies[2] could be overestimated by 7.8 %, since hardwater systems are underrepresented in current modeling and budgets. These estimates apply mean CH_4 flux rates, compiled largely from freshwater sites, to the global lentic area. Yet, we tentatively estimate that 12.8 % of the global area of small-sized waterbodies is salt-rich (166,120 km^2), with an inherently lower emission rate (details in methods). Assuming the total CH_4 emission rate of this fraction of the aquatic area is 2.15 mmol m^{-2} d^{-1} (measured mean in our hardwater survey) instead, yields annual emissions of only 2.1 vs 13.9 $TgCH_4$ yr^{-1} in the current budget. This 11.8 $TgCH_4$ yr^{-1} difference represents a potential overestimation equal to 7.8 % of global lentic CH_4 emissions. This discrepancy highlights the need to better characterize the salinity-CH_4 link

and constrain emissions from hardwater systems, which could ultimately help resolve some of the discrepancy between top-down and bottom-up global CH_4 flux budgets[53].

Future salinization

Worldwide, SO_4^{2-} pollution of inland waters is on the rise due to anthropogenic activities (mining, agriculture, urbanization, atmospheric deposition, climate change)[31,42,54–60], which may further reduce aquatic CH_4 emissions[31]. In the Canadian Prairies, SO_4^{2-} concentrations have increased in 64 % of the 14 monitored lakes for which data are available over the past 30 years (Fig. S4). This is consistent with previous findings that, despite high-local variability, Prairie waters are generally becoming more saline[42,61]. A salinization trend was reported in several regions worldwide[59,60,62], further emphasizing the need to examine the link between CH_4 and ionic composition in different landscapes. Future global increases in temperature, eutrophication, and DOC content, expected to stimulate CH_4 production[34,36,63], may be counteracted by increases in salinity. To derive more accurate predictions, future emissions scenarios should consider changes in salinity along side other key variables and their interactive effects on aquatic CH_4 cycling.

Acknowledgments

This study was funded by a MITACS-Accelerate grant with Ducks Unlimited Canada, awarded to CS in collaboration with LEB and MJB, and a postdoctoral fellowship from the National Scientific and Engineering Research Council (NSERC) to CS. M.J.B was funded by awards from the University of Lethbridge, NSERC, Canada Foundation for Innovation (CFI) and the Canada Research Chairs (CRC) program. PRL was funded by the CRC and CFI programs, NSERC, the

Province of Saskatchewan, and the University of Regina. KF was funded by the Government of Saskatchewan (grant no. 200160015) and NSERC. BW was funded by NSERC (Discovery Grant) and the Saskatchewan Ministry of Environment Fish and Wildlife Development fund. We thank David Butman and Lisa Windham-Myers for important discussions related to data analysis and interpretation.

Author contribution

CS and MJB conceived the study, and LEB and KF contributed to the ideas and conceptualization of the research. Data collection in the field and laboratory was conducted by MJB, LEB, SJ, KF, and PM. MJB, KF, LEB, PRL, and BW provided materials. CS curated and analyzed the data and wrote the original draft of the manuscript. All authors provided input and participated in the manuscript editing and revision process.

221 # Materials and methods

222 ## Sampling sites

223 The study was conducted in the Canadian Prairie ecozone of the provinces of Alberta and
224 Saskatchewan, covering 467,029 km^2 (Fig. S1). The region is characterized by a cold continental
225 to semi-arid climate[64], with extreme seasonal temperature variability (monthly means from ~ 19
226 °C in July to ~ -18 °C in January[32], low annual precipitation, and strong winds[65]. Land use is
227 largely agricultural, containing > 80% of Canada's farmland area[66]. The region is known for its
228 generally flat topography[32,65], widespread endorheic drainage basins, and high evaporation to
229 precipitation ratio, making hardwater lentic systems (wetlands, ponds, and lakes) largely dominant
230 in the regional aquatic landscape[32,40,41]. The region exhibits the highest abundance and diversity of
231 salt-rich lakes worldwide[32], mostly driven by elevated concentrations of SO_4^{2-} (Fig. S2)[32].

232 The survey covered a diverse range of system types and sizes, with 23 sampled rivers, 17
233 lakes, 45 wetlands (shallow open water), and 108 agricultural ponds (Fig. S1 and Table S1), which
234 are common features on the landscape[67]. Each site was sampled once in the summer (June to
235 August, 2011 to 2021).

236

237 ## Environmental parameters

238 At each site, water temperature, dissolved oxygen concentration, pH, and specific
239 conductivity were measured using a multiparameter probe. Salinity was either directly measured
240 by the probe or derived from specific conductivity and temperature using the function 'swSCTp'
241 from the package 'oce'[68] in R[69]. Water samples were collected at each sampling site (at < 0.5m

depth) in clean bottles and stored at cold temperatures until analyzed for DOC, TP, and TN concentrations. DOC analyses were performed on water samples filtered to 0.45 μm on site or in the lab (shortly after collection), then acidified (to remove inorganic carbon) before being processed on an organic carbon analyzer (Shimadzu TOC-L or 5000A, or Aurora 1030W). TP was analyzed by spectrophotometry on a Lachat QuickChem 8500 instrument using the standard molybdenum blue technique after persulfate digestion. TN was measured after chemical digestion on an Alpkem analyzer (IO analytical Flow Solution 3100), a Lachat QuickChem 8500, or a Dionex DX600 instrument. For some sites, TP and TN analysis were performed on filtered samples (0.45 μm) and thus represent the dissolved rather than the total P and N concentrations. However, where both the dissolved and total concentrations were measured, the dissolved fraction represented the vast majority of nutrient content (mean of 77 and 89% for P and N respectively). Therefore, we assumed the dissolved fraction to be representative of the total nutrient content in these samples. The small error that this introduces in the data was considered in the interpretation of results. Chlorophyll *a* concentration was measured in most lentic systems by spectrophotometry after filtration (on GF/F or GF/C filters) and alcohol extraction. Concentration of SO_4^{2-} was measured in 118 sites using a SmartChem 200 discrete analyzer or a Dionex DX600 and ICS2500. River discharge data at time of sampling were obtained via the National Hydrological Services of Canada, and directly from both the Saskatchewan Watershed Authority and Alberta Environment and Parks. Stream velocity was estimated based on discharge following the relationship in Campeau & Del Giorgio (2014)[37].

CH_4 partial pressure and flux

CH_4 concentration in all samples was determined using the headspace technique, however, since the database is a post hoc combination of data collected independently by different research teams, details of the gas sampling method are not uniform. However, variation introduced by distinct methodologies is expected to be minor relative to the measured range of CH_4 content across sites. Overall, water was collected in an airtight container (140 mL plastic syringe or 1.2 L glass bottle or 160 mL Wheaton glass serum bottle). An air headspace was created inside the sealed container, either on site or in the laboratory (after preserving the water with potassium chloride). The headspace consisted of ambient air at the sampling site or ultrahigh purity dinitrogen in the laboratory, and the air to water ratio varied between 0.05 and 0.25. To equilibrate the gas and water phases, the closed container was shaken for at least 2 min. The gas phase was then extracted and analyzed for CH_4 concentration by gas chromatography on a GC Scion 456, a Varian 3800, or a Thermo Trace 1310 instrument, calibrated against multiple standards. The in-situ concentration of CH_4 in the water was back-calculated based on the gas solubility (dependent on salinity and water temperature) before and after equilibration, local atmospheric pressure, and the headspace air to water ratio.

Surface CH_4 diffusive flux rates to the atmosphere were calculated in 139 wetlands and ponds using the following equation:

$$F = k\,(C_{eq} - C_w) \qquad \text{(Eq. 1)}$$

Where F is the CH_4 diffusive flux rate, k is the air-water gas transfer velocity, C_{eq} is the CH_4 concentration in the water at equilibrium, and C_w is the CH_4 concentration measured in the water. The parameter k was estimated based on an empirical wind-based model[70]:

286 $$k_{600} = 2.07 + 0.215\, U_{10}^{1.7}$$ (Eq. 2)

287 with k_{600} the normalized gas transfer velocity (converted to a CH_4 specific k using the Schmidt
288 number with an exponent of 0.67[70]), and U_{10} the average mean wind speed at 10 m at the time of
289 sampling across sites. Direct floating chamber measurements were performed in a subset of 10
290 ponds as described in a previous study[71].

291 CH_4 ebullition flux rates were measured at 10 sites (5 natural wetlands and 5 agricultural
292 ponds). In each site, bubbles were collected by deploying two inverse funnel traps (0.061 m^2 and
293 27.3 cm diameter), one in the shallow and one in the deep region of the waterbody, sampled at
294 least 3 times from June to August to determine the volume of bubbles emitted. The CH_4 content of
295 bubbles upon ascension was determined by perturbing the sediments and collecting freshly emitted
296 bubbles with funnel traps fitted with an airtight plastic syringe. Gas collected in the syringe was
297 injected in 12 mL Labco vials and analyzed for CH_4 concentration as above. Summer mean CH_4
298 ebullition rate was calculated for each site as the product of the total volume of bubble emitted and
299 the concentration of CH_4 in freshly emitted bubbles, converted to an areal daily flux rate (per m^2
300 of surface water).

301

302 **Statistical analyses**

303 All statistical analyses were performed in R[69]. Prior to analysis, data were $\log_{10}$ transformed
304 if necessary to meet normality requirements. The links between pCH_4 or flux and other variables
305 were assessed via multiple linear regressions using the function 'lm', and verifying the
306 homoscedasticity of the residuals with a Shapiro-Wilk test (function 'shapiro.test'). The same

regression analysis was performed on standardized values (to a standard deviation of one) to compare effect sizes (coefficients) of explanatory variables (Fig. S2). A marginal effect analysis was performed for each system type using the R package 'sjPlot'[72] to visualize the effect of salinity on pCH_4 when other variables are held constant (at dataset average).

Measured pCH_4, diffusive, and ebullitive fluxes were compared to predicted values based on existing literature models. We selected multiple models that use established CH_4 predictors measured in our dataset, and that are based on empirical surveys in Canada or at the global scale. pCH_4 was modeled based on surface area, temperature, and TN for lentic systems (lakes, wetlands, and ponds)[35], and on temperature, velocity, and DOC concentration for lotic systems[37]. Both models are based on empirical linear relationships developed from large-scale surveys in the eastern Canada[35,37]. Predicted CH_4 diffusive flux rate was calculated as the mean of two modeled values: a global model using area and Chl *a* concentration[5], and a regional East-Canadian model using area and temperature[35]. Likewise, predicted CH_4 ebullition was considered as the mean of a global model based on a global relationship with Chl *a*[5], and a regional (East-Canada) model using sediment temperature[34]. The use of multiple models allows us to account for multiple controls of CH_4 and reduce the bias associated with one particular model.

Spatial upscaling

To estimate the effect of salinity on CH_4 emissions at a regional scale, we simulated CH_4 total flux rate using the regression model developed in Fig. 4 as a function of two salinity levels: 0.5 ppt (median of sampled small lentic sites) vs 0.1 ppt (typical value in freshwaters). The regression model is based on 10 sites (5 wetlands and 5 ponds) with robust data on both diffusive

329 and ebullitive summer fluxes, providing well constrained total CH_4 emissions from open-water
330 environments (excluding emergent vegetation). The difference in CH_4 flux rate between the two
331 scenarios was applied to three months of summer (91 days) and to the regional surface area covered
332 by small lentic waterbodies. We calculated the lentic surface area of the Canadian Prairie ecozone
333 using a combination of geospatial layers: the Canadian Wetland Inventory (CWI)[73], and the
334 Alberta Biodiversity Monitoring Institute / Ducks Unlimited Canada Southern Saskatchewan
335 Moderate Resolution Wetland Inventory (ABMI/DUC 2022; systems ≥ 0.0004 km^2)[74] for areas
336 outside of the CWI layer coverage (45.9 %). We selected waterbodies of 'shallow/open-water'
337 type and filtered out riverine wetlands (to exclude floodplains) to get a conservative areal estimate
338 of lentic waterbodies of 8,843 km^2, representing 1.9% of regional land cover. We restricted the
339 upscaling exercise to lentic systems smaller than 0.1 km^2 (totalling 2,869 km^2) to remain in the
340 size range of our empirical model. The product of this regional aquatic area by the difference in
341 CH_4 flux rate in hardwater vs freshwater scenarios represented the potential overestimation of CH_4
342 emissions from small waterbodies of the Canadian Prairies if these systems were considered as
343 salt-poor (0.1 ppt).

344 To assess the salt effect on CH_4 flux at a global scale, we estimated the global area of salt-
345 rich small lentic systems and calculated their emissions based on the current CH_4 budget[2] vs a
346 lower mean flux rate derived from our hardwater measurements. The area of 166,120 km^2 was
347 derived from the tentative lower-bound estimate of the global area of salt-rich inland waters
348 (538,892 km^2)[75] multiplied by 0.31, the fraction of small (< 0.1 km^2) systems based on the global
349 size distribution of lakes[76]. The most recent budget estimates the annual emissions of small lentic
350 systems (< 0.1 km^2) to be 108 $TgCH_4\ yr^{-1}$ [2], from which 13.9 $TgCH_4\ yr^{-1}$ is attributed to salt-rich
351 systems, assuming the fraction of salt-rich to total area of small lentic systems is 12.8 %[75,76]. We

recalculated emission of this subset of systems by applying the average total CH_4 flux rate measured in our hardwater study sites (2.15 mmol m^{-2} d^{-1}) to the estimated global area of small salt-rich waterbodies, yielding 2.1 $TgCH_4$ yr^{-1}. The difference between the two values (13.9 – 2.1 $TgCH_4$ yr^{-1}) was considered as the potential overestimation of emissions in the global aquatic CH_4 budget when not explicitly considering the lower emission rate due to salinity in hardwater systems.

Temporal trends

To explore temporal trends in SO_4^{2-} concentration in the study region, we used a publicly available (Saskatchewan Water Security Agency), long-term monitoring dataset collected in southern Saskatchewan lentic systems between 1990 and 2020. A subset of sites was selected for long-term trend analysis based on the following criteria: 1) a minimum of 10 observations within the 1990 - 2020 time period, 2) observations span at least 5 years, 3) at least one recent observation after 2010. Where all three criteria were met, a Sen slope analysis was performed using R package 'zyp'[77] to determine the trends in SO_4^{2-} over the past 3 decades. For each Sen slope, a 95 % confidence interval (CI) was calculated and used to determine the significance of the slope, with trends considered significantly increasing or decreasing if the CI range was entirely positive or negative respectively (Fig. S4).

References

1. Ciais, P. *et al.* Carbon and Other Biogeochemical Cycles. *Clim. Chang. 2013 - Phys. Sci. Basis* 465–570 (2013) doi:10.1017/CBO9781107415324.015.

2. Rosentreter, J. A. *et al.* Half of global methane emissions come from highly variable aquatic ecosystem sources. *Nat. Geosci.* **14**, 225–230 (2021).

3. Saunois, M. *et al.* The global methane budget 2000-2017. *Earth Syst. Sci. Data* **12**, 1561–1623 (2020).

4. Deemer, B. R. *et al.* Greenhouse Gas Emissions from Reservoir Water Surfaces: A New Global Synthesis. *Bioscience* **66**, 949–964 (2016).

5. DelSontro, T., Beaulieu, J. J. & Downing, J. A. Greenhouse gas emissions from lakes and impoundments: Upscaling in the face of global change. *Limnol. Oceanogr. Lett.* **3**, 64–75 (2018).

6. Stanley, E. H. *et al.* The ecology of methane in streams and rivers: patterns, controls, and global significance. *Ecol. Monogr.* **86**, 146–171 (2016).

7. Waiser, M. J. & Robarts, R. D. Saline Inland Waters. in *Encyclopedia of Inland Waters* 634–644 (Elsevier, 2009). doi:10.1016/B978-012370626-3.00028-4.

8. Camacho, A. *et al.* Methane emissions in Spanish saline lakes: Current rates, temperature and salinity responses, and evolution under different climate change scenarios. *Water (Switzerland)* **9**, 1–20 (2017).

9. Poffenbarger, H. J., Needelman, B. A. & Megonigal, J. P. Salinity influence on methane

392 emissions from tidal marshes. *Wetlands* **31**, 831–842 (2011).

393 10. Pennock, D. *et al.* Landscape controls on N2O and CH4 emissions from freshwater
394 mineral soil wetlands of the Canadian Prairie Pothole region. *Geoderma* **155**, 308–319
395 (2010).

396 11. Lovley, D. R. & Phillips, E. J. P. Competitive Mechanisms for Inhibition of Sulfate
397 Reduction and Methane Production in the Zone of Ferric Iron Reduction in Sediments.
398 *Appl. Environ. Microbiol.* **53**, 2636–2641 (1987).

399 12. Yang, J., Ma, L., Jiang, H., Wu, G. & Dong, H. Salinity shapes microbial diversity and
400 community structure in surface sediments of the Qinghai-Tibetan Lakes. *Sci. Rep.* **6**, 6–11
401 (2016).

402 13. Deng, Y., Liu, Y., Dumont, M. & Conrad, R. Salinity Affects the Composition of the
403 Aerobic Methanotroph Community in Alkaline Lake Sediments from the Tibetan Plateau.
404 *Microb. Ecol.* **73**, 101–110 (2017).

405 14. Liu, Y. *et al.* Salinity drives archaeal distribution patterns in high altitude lake sediments
406 on the Tibetan Plateau. *FEMS Microbiol. Ecol.* **92**, 1–10 (2016).

407 15. Sivan, O., Shusta, S. S. & Valentine, D. L. Methanogens rapidly transition from methane
408 production to iron reduction. *Geobiology* **14**, 190–203 (2016).

409 16. Van Bodegom, P. M., Scholten, J. C. M. & Stams, A. J. M. Direct inhibition of
410 methanogenesis by ferric iron. *FEMS Microbiol. Ecol.* **49**, 261–268 (2004).

411 17. Zehnder, A. J. B. B. & Brock, T. D. Anaerobic methane oxidation: Occurrence and

412 ecology. *Appl. Environ. Microbiol.* **39**, 194–204 (1980).

413 18. Baldwin, D. S. & Mitchell, A. Impact of sulfate pollution on anaerobic biogeochemical
414 cycles in a wetland sediment. *Water Res.* **46**, 965–974 (2012).

415 19. Raghoebarsing, A. A. *et al.* A microbial consortium couples anaerobic methane oxidation
416 to denitrification. *Nature* **440**, 918–921 (2006).

417 20. Valentine, D. L. & Reeburgh, W. S. New perspectives on anaerobic methane oxidation.
418 *Environ. Microbiol.* **2**, 477–484 (2000).

419 21. Kleint, J. F., Wellach, Y., Schroll, M., Keppler, F. & Isenbeck-Schröter, M. The impact of
420 seasonal sulfate–methane transition zones on methane cycling in a sulfate-enriched
421 freshwater environment. *Limnol. Oceanogr.* 1–19 (2021) doi:10.1002/lno.11754.

422 22. La, W. *et al.* Sulfate concentrations affect sulfate reduction pathways and methane
423 consumption in coastal wetlands. *Water Res.* **217**, 118441 (2022).

424 23. Mostovaya, A., Wind-Hansen, M., Rousteau, P., Bristow, L. A. & Thamdrup, B. Sulfate-
425 and iron-dependent anaerobic methane oxidation occurring side-by-side in freshwater lake
426 sediment. *Limnol. Oceanogr.* **67**, 231–246 (2022).

427 24. Dalcin Martins, P. *et al.* Abundant carbon substrates drive extremely high sulfate
428 reduction rates and methane fluxes in Prairie Pothole Wetlands. *Glob. Chang. Biol.* **23**,
429 3107–3120 (2017).

430 25. Chamberlain, S. D. *et al.* Effect of Drought-Induced Salinization on Wetland Methane
431 Emissions, Gross Ecosystem Productivity, and Their Interactions. *Ecosystems* **23**, 675–

688 (2020).

26. van Dijk, G. *et al.* Salinization lowers nutrient availability in formerly brackish freshwater wetlands; unexpected results from a long-term field experiment. *Biogeochemistry* **143**, 67–83 (2019).

27. Bansal, S., Tangen, B. & Finocchiaro, R. Temperature and Hydrology Affect Methane Emissions from Prairie Pothole Wetlands. *Wetlands* **36**, 371–381 (2016).

28. van Dijk, G. *et al.* Salinization of coastal freshwater wetlands; effects of constant versus fluctuating salinity on sediment biogeochemistry. *Biogeochemistry* **126**, 71–84 (2015).

29. Vizza, C., West, W. E., Jones, S. E., Hart, J. A. & Lamberti, G. A. Regulators of coastal wetland methane production and responses to simulated global change. *Biogeosciences* **14**, 431–446 (2017).

30. Chambers, L. G., Osborne, T. Z. & Reddy, K. R. Effect of salinity-altering pulsing events on soil organic carbon loss along an intertidal wetland gradient: A laboratory experiment. *Biogeochemistry* **115**, 363–383 (2013).

31. Gauci, V. *et al.* Sulfur pollution suppression of the wetland methane source in the 20th and 21st centuries. *Proc. Natl. Acad. Sci. U. S. A.* **101**, 12583–12587 (2004).

32. Last, W. M. & Ginn, F. M. Saline systems of the Great Plains of western Canada: an overview of the limnogeology and paleolimnology. *Saline Systems* **1**, 10 (2005).

33. Yvon-Durocher, G. *et al.* Methane fluxes show consistent temperature dependence across microbial to ecosystem scales. *Nature* **507**, 488–91 (2014).

34. DelSontro, T., Boutet, L., St-Pierre, A., del Giorgio, P. A. & Prairie, Y. T. Methane ebullition and diffusion from northern ponds and lakes regulated by the interaction between temperature and system productivity. *Limnol. Oceanogr.* **61**, S62–S77 (2016).

35. Rasilo, T., Prairie, Y. T. & Del Giorgio, P. A. Large-scale patterns in summer diffusive CH4 fluxes across boreal lakes, and contribution to diffusive C emissions. *Glob. Chang. Biol.* **1**, 1–16 (2014).

36. Beaulieu, J. J., DelSontro, T. & Downing, J. A. Eutrophication will increase methane emissions from lakes and impoundments during the 21st century. *Nat. Commun.* **10**, 3–7 (2019).

37. Campeau, A. & Del Giorgio, P. A. Patterns in CH4 and CO2 concentrations across boreal rivers: Major drivers and implications for fluvial greenhouse emissions under climate change scenarios. *Glob. Chang. Biol.* **20**, 1075–1088 (2014).

38. Li, M. *et al.* The significant contribution of lake depth in regulating global lake diffusive methane emissions. *Water Res.* **172**, 115465 (2020).

39. Günthel, M. *et al.* Contribution of oxic methane production to surface methane emission in lakes and its global importance. *Nat. Commun.* (2019) doi:10.1038/s41467-019-13320-0.

40. van der Valk, A. G. & Pederson, R. L. The SWANCC decision and its implications for prairie potholes. *Wetlands* **23**, 590–596 (2003).

41. Webb, J. R. *et al.* Widespread nitrous oxide undersaturation in farm waterbodies creates

an unexpected greenhouse gas sink. *Proc. Natl. Acad. Sci.* **116**, 9814–9819 (2019).

42. Kerr, J. G. Multiple land use activities drive riverine salinization in a large, semi-arid river basin in western Canada. *Limnol. Oceanogr.* **62**, 1331–1345 (2017).

43. Bailey, L. D. The sulphur status of eastern Canadian prairie soils: the relationship of sulphur, nitrogen and organic carbon. *Can. J. Soil Sci.* **65**, 179–186 (1985).

44. Hinckley, E.-L. S., Crawford, J. T., Fakhraei, H. & Driscoll, C. T. A shift in sulfur-cycle manipulation from atmospheric emissions to agricultural additions. *Nat. Geosci.* **13**, 597–604 (2020).

45. Pham, S. V., Leavitt, P. R., McGowan, S., Wissel, B. & Wassenaar, L. I. Spatial and temporal variability of prairie lake hydrology as revealed using stable isotopes of hydrogen and oxygen. *Limnol. Oceanogr.* **54**, 101–118 (2009).

46. Mitchell, M. J., Driscoll, C. T., McHale, P. J., Roy, K. M. & Dong, Z. Lake/watershed sulfur budgets and their response to decreases in atmospheric sulfur deposition: watershed and climate controls. *Hydrol. Process.* **27**, 710–720 (2013).

47. Hotchkiss, E. R., Sadro, S. & Hanson, P. C. Toward a more integrative perspective on carbon metabolism across lentic and lotic inland waters. *Limnol. Oceanogr. Lett.* **1204964**, 57–63 (2018).

48. Sereda, J., Bogard, M., Hudson, J., Helps, D. & Dessouki, T. Climate warming and the onset of salinization: Rapid changes in the limnology of two northern plains lakes. *Limnologica* **41**, 1–9 (2011).

492 49. Aguirrezabala-Campano, T., Gerardo-Nieto, O., Gonzalez-Valencia, R., Souza, V. &
493 Thalasso, F. Methane dynamics in the subsaline ponds of the Chihuahuan Desert: A first
494 assessment. *Sci. Total Environ.* **666**, 1255–1264 (2019).

495 50. Yan, F. *et al.* Lakes on the Tibetan Plateau as Conduits of Greenhouse Gases to the
496 Atmosphere. *J. Geophys. Res. Biogeosciences* **123**, 2091–2103 (2018).

497 51. Chen, Z. *et al.* Assessment of regional greenhouse gas emission from beef cattle
498 production: A case study of Saskatchewan in Canada. *J. Environ. Manage.* **264**, 110443
499 (2020).

500 52. Environment and Climate Change Canada. *2019 National Inventory Report (NIR) - Part 1*.
501 (2021).

502 53. Etiope, G. & Schwietzke, S. Global geological methane emissions: An update of top-down
503 and bottom-up estimates. *Elem. Sci. Anthr.* **7**, 1–9 (2019).

504 54. Herbert, E. R. *et al.* A global perspective on wetland salinization: Ecological
505 consequences of a growing threat to freshwater wetlands. *Ecosphere* **6**, 1–43 (2015).

506 55. Kaushal, S. S. *et al.* Novel 'chemical cocktails'' in inland waters are a consequence of the
507 freshwater salinization syndrome'. *Philos. Trans. R. Soc. B Biol. Sci.* **374**, 20180017
508 (2019).

509 56. Cañedo-Argüelles, M., Kefford, B. & Schäfer, R. Salt in freshwaters: causes, effects and
510 prospects - introduction to the theme issue. *Philos. Trans. R. Soc. B Biol. Sci.* **374**,
511 20180002 (2019).

512 57. Hinckley, E.-L. S. L. S., Crawford, J. T., Fakhraei, H. & Driscoll, C. T. A shift in sulfur-
513 cycle manipulation from atmospheric emissions to agricultural additions. *Nat. Geosci.* **13**,
514 597–604 (2020).

515 58. Zak, D. *et al.* Sulphate in freshwater ecosystems: A review of sources, biogeochemical
516 cycles, ecotoxicological effects and bioremediation. *Earth-Science Rev.* **212**, (2021).

517 59. Jeppesen, E., Beklioğlu, M., Özkan, K. & Akyürek, Z. Salinization Increase due to
518 Climate Change Will Have Substantial Negative Effects on Inland Waters: A Call for
519 Multifaceted Research at the Local and Global Scale. *Innov.* **1**, 1–2 (2020).

520 60. Thorslund, J., Bierkens, M. F. P., Oude Essink, G. H. P., Sutanudjaja, E. H. & van Vliet,
521 M. T. H. Common irrigation drivers of freshwater salinisation in river basins worldwide.
522 *Nat. Commun.* **12**, (2021).

523 61. Nachshon, U., Ireson, A., Van Der Kamp, G., Davies, S. R. & Wheater, H. S. Impacts of
524 climate variability on wetland salinization in the North American prairies. *Hydrol. Earth*
525 *Syst. Sci.* **18**, 1251–1263 (2014).

526 62. Stets, E. G. *et al.* Landscape Drivers of Dynamic Change in Water Quality of U.S. Rivers.
527 *Environ. Sci. Technol.* **54**, 4336–4343 (2020).

528 63. Pagano, T., Bida, M. & Kenny, J. Trends in Levels of Allochthonous Dissolved Organic
529 Carbon in Natural Water: A Review of Potential Mechanisms under a Changing Climate.
530 *Water* **6**, 2862–2897 (2014).

531 64. Peel, M. C., Finlayson, B. L. & McMahon, T. A. Updated world map of the Köppen-

Geiger climate classification. *Hydrol. Earth Syst. Sci.* **11**, 1633–1644 (2007).

65. McGinn, S. M. Weather and climate patterns in Canada's prairie grasslands. *Arthropods Can. Grasslands (Volume 1) Ecol. Interact. Grassl. Habitats* 105–119 (2010) doi:10.3752/9780968932148.ch5.

66. Environment and Climate Change Canada. Introduction - Prairies. https://www.nrcan.gc.ca/changements-climatiques/impacts-adaptation/introduction-prairies/10381#table4 (2015).

67. Yew Gan, T. Reducing Vulnerability of Water Resources of Canadian Prairies to Potential Droughts and Possible Climatic Warming. *Water Resour. Manag.* **14**, 111–135 (2000).

68. Kelley, D. E. *Oceanographic Analysis with R*. (Springer New York, 2018). doi:10.1007/978-1-4939-8844-0.

69. R Core Team. R: A language and environment for statistical computing. (2017).

70. Cole, J. J. & Caraco, N. F. Atmospheric exchange of carbon dioxide in a low-wind oligotrophic lake measured by the addition of SF6. *Limnol. Oceanogr.* **43**, 647–656 (1998).

71. Webb, J. R. *et al.* Regulation of carbon dioxide and methane in small agricultural reservoirs: Optimizing potential for greenhouse gas uptake. *Biogeosciences Discuss.* 1–24 (2019) doi:10.5194/bg-2019-263.

72. Ludecke, D. sjPlot: Data Visualization for Statistics in Social Science. (2018).

73. Canadian Wetland Inventory Technical Committee. Canadian Wetland Inventory (Data

Model) version 7.0. 36 (2016).

74. ABMI. *ABMI Wetland Inventory*. *Alberta Biodiversity Monitoring Institute* https://abmi.ca/home/data-analytics/da-top/da-product-overview/Advanced-Landcover-Prediction-and-Habitat-Assessment--ALPHA--Products/ABMI-Wetland-Inventory.html (2021).

75. Finlay, K. *et al.* Decrease in CO2 efflux from northern hardwater lakes with increasing atmospheric warming. *Nature* **519**, 215–218 (2015).

76. Downing, J. A. *et al.* The global abundance and size distribution of lakes, ponds, and impoundments. *Limnol. Oceanogr.* **51**, 2388–2397 (2006).

77. Bronaugh, D. & Werner, A. Zhang + Yue-Pilon Trends Package. (2019).

Supplementary Files

This is a list of supplementary files associated with this preprint. Click to download.

- Souedetalsalinitych4SIv4.pdf